International Immunopharmacology 73 (2019) 515–526

Contents lists available at ScienceDirect

International Immunopharmacology

journal homepage: www.elsevier.com/locate/intimp

Inhibitory effects of octreotide on the progression of hepatic fibrosis via the regulation of Bcl-2/Bax and PI3K/AKT signaling pathways

Chong Zhang[a,1], Ran An[b,1], Ya-Wei Bao[c,1], Xiao-Ming Meng[d], Tian-Qi Wang[a], Hao-Nan Sun[a], Fa-Ming Pan[e], Chao Zhang[a,*]

[a] Department of Hepatobiliary Surgery, The First Affiliated Hospital of Anhui Medical University, Hefei, China
[b] Department of Emergency Surgery, The First Affiliated Hospital of Anhui Medical University, Hefei, China
[c] Department of Plastic Surgery, The First Affiliated Hospital of Anhui Medical University, Hefei, China
[d] School of Pharmacy, Anhui Key Laboratory of Bioactivity of Natural Products, Anhui Medical University, Hefei, China
[e] Department of Epidemiology and Statistics, School of Public Health, Anhui Medical University, Hefei, China

ARTICLE INFO

Keywords:
Octreotide
Liver fibrosis
PI3K
AKT
Bcl-2
Bax

ABSTRACT

In a previous study, we showed that octreotide alleviate hepatic fibrosis. However, its underlying molecular mechanisms are still poorly understood. In the current study, rats with CCl_4-induced liver injury and Hepatic Stellate Cells (HSCs) were employed for in vitro and in vivo studies to observe the effects of octreotide on progression of liver fibrosis. The results in rats indicated that octreotide remarkably alleviated hepatic injury. The treated rats showed improved pathological manifestations and reduced liver indicators, e.g., liver weight, liver index and liver hydroxyproline (Hyp) content. Additionally, activities of serum total bilirubin (TBIL), aspartate transaminase (AST) and alanine transaminase (ALT), and serum levels of hyaluronic acid (HA), laminin (LN), type IV collagen (IV-C) and procollagen III peptide (PIIIP) also decreased. Furthermore, releasing inflammatory factors and proliferation of activated HSCs under different treatments were detected in which levels of IL-1β, IL-6, TNF-α decreased and hepatocytes proliferative capacity reduced through Bcl-2/Bax-dependent apoptosis. Finally, our results demonstrated that octreotide was able to exert an inhibitory effect on the activation of HSCs regulating the PI3K/AKT signaling pathway. In summary, our study corroborated that octreotide could prevent liver fibrosis probably via modulating Bcl-2/Bax and PI3K/AKT signaling pathway.

1. Introduction

Hepatic fibrosis is a dynamic wound-healing process in which the liver responds to a series of chronic liver injuries, including viral infection, alcohol consumption, cholestasis, autoimmune diseases and non-alcoholic steatohepatitis [1,2]. It is well known that the activation of hepatic stellate cells (HSCs) plays a key role in liver fibrogenesis [3,4]. In normal liver tissue, HSCs remain quiescent within the perisinusoidal space and keep the balance of the basal membrane matrix. Correspondingly, HSCs would secrete a variety of pro-inflammatory factors and extracellular matrix (ECM) proteins after activation leading to the progression of liver fibrosis [5–7]. It is reported that damaged hepatocytes are able to induce activation of HSCs by virtue of releasing multiple fibrogenic cytokines and inflammatory factors [8]. Hence, it is recommended to inhibit the release of fibrogenic cytokines and inflammatory factors and the proliferation of activated HSCs, which may represents a potential strategy for the treatment of liver fibrosis.

Recently, several studies have investigated the mechanisms of liver fibrosis, which indicate that PI3K/AKT signaling is closely associated with the activation, proliferation and ECM synthesis of HSCs [9,10]. Additionally, it has been reported that the inhibition of PI3K/AKT signaling via genetic and pharmacological methods suppresses the activation of HSCs [11,12]. Biologically, the Bcl-2/Bax signaling pathway is also estimated to be involved in the progression of hepatic fibrosis through cell apoptosis pathway [13,14]. Bcl-2 and Bax, as the members of Bcl-2 family, play an important role in apoptosis by modulating mitochondrial outer membrane permeability [15]. It has also been reported that Bcl-2/Bax signaling pathway could exert dual effects in hepatocyte and activated HSCs in which hepatocyte apoptosis promotes hepatic fibrosis and activated HSC apoptosis alleviates hepatic fibrosis [16–18].

Somatostatin and its analogue, octreotide, are known to inhibit DNA

* Corresponding author at: Department of Hepatobiliary Surgery, The First Affiliated Hospital of Anhui Medical University, Hefei 230022, China.
E-mail address: 13965053990@163.com (C. Zhang).
[1] These authors contributed equally to this work.

https://doi.org/10.1016/j.intimp.2019.05.055
Received 27 January 2019; Received in revised form 26 May 2019; Accepted 28 May 2019
Available online 04 June 2019
1567-5769/

synthesis and proliferation of activated HSCs [19]. Previous studies have demonstrated that somatostatin exerted its inhibitive action on activated HSCs by means of somatostatin receptors subtypes (SSTRs), especially SSTR2 [20]. Meanwhile, there were studies demonstrated that octreotide could alleviate liver fibrosis through the inhibitory effect on the activation of HSCs by down-regulating the expression of transforming growth factor (TGF)-β [21]. Our previous study found that octreotide could attenuate liver fibrosis by inhibiting the Wnt/β-catenin signaling pathway [22]. However, further mechanisms underlying the protective effect of octreotide on liver fibrosis remain to be explored.

In summary, the present study aims to investigate the effects of octreotide on the progression of liver fibrosis through in vivo and in vitro experiments and to evaluate inflammation, HSC activation, apoptosis and their relevant signaling pathways to illustrate orchestrated mechanism of the antifibrosis effect of octreotide.

2. Materials and methods

2.1. Animal models

Male Sprague-Dawley rats (180-200 g) were obtained from the Experimental Animal Center of Anhui Medical University (Hefei, Anhui, China). All animal experimental procedures were approved by the Anhui Medical University Committee on the Care and Use of Animals. All rats were housed under a 12 h light/dark cycle at 20–24 °C and humidity was 40%–60% with free access to food and water.

Thirty rats were divided randomly into three groups: control group, model group and octreotide group. Rats in the model group and the octreotide group were subcutaneously injected with CCl_4 was diluted into 40% (v/v) in olive oil at a dose of 3 mL/kg twice a week for 8 weeks to induce liver fibrosis. Meanwhile, rats in the octreotide group were hypodermically injected with octreotide (Novartis Pharma AG, Basel, Switzerland) diluted with saline (10 μg/kg) twice a day for 8 weeks. Rats in the control group were received with the same volume of olive and saline at the same time intervals. Our pilot study showed that octreotide had no toxicity at the dose of 10 μg/kg (data are not shown). At the end of the experiment, all rats were anesthetized with 10% chloral hydrate and sacrificed. Blood was collected and centrifuged (1000 × *g* for 15 min) to determine the serum biochemical parameters, and liver tissues were harvested to calculate the liver index. The liver samples in each group were fixed with 10% formalin, and the other parts of the liver tissue were stored at −80 °C.

2.2. Calculation of liver index

The liver index was calculated as the following formula: $\text{Liver index} = \frac{\text{liver weight}}{\text{body weight}} \times 100\%$.

2.3. Primary HSCs isolation

Primary HSCs were extracted via collagenase-pronase perfusion followed by centrifugation in a Nycodenz solution. The portal vein was severed and inserted by special needle. Perfusion buffer perfused liver via portal vein. After the blood was washed away by perfusion buffer and then liver turned to white, the liver was perfused with enzymes fix (sigma, GER) until liver was digested completely. The liver was carefully removed from the abdominal cavity and minced under sterile condition. Then the liver was disrupted to obtain cell suspension which was filtered to remove undigested debris. Cell suspension was centrifuged by several times, and the cell suspension density was adjusted with Nycodenz mixture. Primary HSCs were collected by the gradient centrifugation.

2.4. Cell culture and treatment

The LX-2 cell line, immortalized human HSC line, was donated by Dr. Scott Friedman (Mount Sinai School of Medicine, USA). LX-2 cells were cultured and maintained at 37 °C in a humidified atmosphere containing 5% CO_2 on Dulbecco's modified Eagle's medium (DMEM, Gibco, USA) supplemented with 10% fetal bovine serum (FBS, Gibco, USA), 100 U/mL penicillin and 100 U/mL streptomycin. Cells were divided into five groups and plated in 6-well plates and 96-well plates and incubated for western blot analysis, real-time PCR analysis and cell proliferation analysis as follows: 1) normal group: cells with DMEM only; 2) control group: cells with DMEM containing TGF-β1 (10 ng/mL); 3) octreotide group: cells with DMEM containing TGF-β1 (10 ng/mL) and octreotide (1×10^{-8} mol/L, 1×10^{-7} mol/L and 1×10^{-6} mol/L).

2.5. Cell proliferation analysis

Cell proliferation was measured using a 3-(4, 5-dimethylthiazol-2-yl)-2, 5-diphenyltetrazolium bromide (MTT) assay. LX-2 cells were seeded into 96-well plates at a density of 5000 cells/well. After stabilization for 24 h, the culture medium was changed and 10 ng/mL TGF-β1 was added to wells of the control group and the octreotide group, incubating for another 24 h. Then, three different concentrations of octreotide in 100 μL of the culture medium (1×10^{-8} mol/L, 1×10^{-7} mol/L and 1×10^{-6} mol/L) were added to the corresponding wells. After incubating for 48 h, 20 μL of MTT at 5 mg/mL was added to each well for an incubation of 4 h. Thereafter, the supernatant was removed and 100 μL dimethylsulfoxide (DMSO) was added to each well and plates were vibrated for 10 min. The optical density (OD) value was measured in enzyme-linked immunity implement (Elx800, Bio-TEK, VT, USA) at 570 nm.

2.6. Histological analysis

Liver tissues were fixed in 10% formalin and embedded in paraffin. After being cut into 5 μm-thick sections, liver tissue sections were stained with hematoxylin-eosin (HE) and Masson's stains for evaluating the changes in liver pathology and collagen deposition. Microscopic fields in liver sections were selected randomly for evaluation and photographed by using an Olympus BX-145 microscope (Olympus, Japan).

2.7. Biochemical analysis

The activities of TBIL, ALT and AST from each serum sample were measured with kits (Jianchenbio, Nanjing, China) according to the manufacturer's protocol. Liver Hyp content was determined by using a hydroxyproline detection kit (Sigma-Aldrich, St. Louis, Mo, USA) according to the manufacturer's protocol. Concentrations of HA, LN, IV-C and PIIIP were measured by radioimmunoassay kits (Beifang Institute of Biotechnology, Beijing, China) according to the manufacturer's protocol.

2.8. Immunohistochemistry staining

The remaining slices with 5 μm sections were deparaffinized and covered with 3% hydrogen peroxide for 20 min at 37 °C to block endogenous peroxidase activity, and washed in phosphate buffered saline (PBS). Antigen repair was performed by heating in sodium citrate buffer (PH 6.0) for 10 min. Sections were further immersed in 2% bovine serum albumin and then incubated with rabbit primary antibody against α-SMA (1:50, Proteintech, No.55135-1-AP, USA), collagen I (1:100, Abcam, ab34710, UK), Bcl-2 (1:300, Abcam, ab32124, UK) and Bax (1:250, Abcam, ab32503, UK) overnight at 4 °C. The next day, after rinsing, the sections were incubated with biotinylated secondary

Table 1
Primer sequence used for RT-PCR.

Target gene	Race	Forward sequence	Reverse sequence
α-SMA	Human	5′-TCATGGTCGGTATGGGTCAG-3′	5′-CCGTGCTCGATAGGGTACTT-3′
	Rat	5′-CAATGGCTCCGGGCTCTGTA-3′	5′-CTCTTGCTCTGCGCTTCGTC-3′
Collagen I	Human	5′-CACCAATCACCTGCGTACAG-3′	5′-GCAGTTCTTGGTCTCGTCAC-3′
	Rat	5′-ACCTCAGGGTATTGCTGGAC-3′	5′-GACCAGGGAAGCCTCTTTCT-3′
Bax	Human	5′-CCCGAGAGGTCTTTTTCCGAG-3′	5′-CCAGCCCATGATGGTTCTGAT-3′
	Rat	5′-AGACACCTGAGCTGACCTTGGAG-3′	5′-GTTGAAGTTGCCATCAGCAAACA-3′
Bcl-2	Human	5′-GGTGGGGTCATGTGTGTGG-3′	5′-CGGTTCAGGTACTCAGTCATCC-3′
	Rat	5′-TGAACCGGCATCTGCACAC-3′	5′-CGTCTTCAGAGACAGCCAGGAG-3′
IL-1β	Human	5′-GGACAAGCTGAGGAAGATGC-3′	5′-TCGTTATCCCATGTGTCGAA-3′
	Rat	5′-TACCTATGTCTTGCCCGTGGAG-3′	5′-ATCATCCCACGAGTCACAGAGG-3′
IL-6	Human	5′-CACACAGACAGCCACTCACC-3′	5′-AGTGCCTCTTTGCTGCTTTC-3′
	Rat	5′-TCACTGTGCGTTGCAAACAGTGTC-3′	5′-ATACCACAAGGTTGGCAGGTGGAT-3′
TNF-α	Human	5′-AACCTCCTCTCTGCCATCAA-3′	5′-CTGAGTCGGTCACCCTTCTC-3′
	Rat	5′-CTTCTGTCTACTGAACTTCGGGGT-3′	5′-TGGAACTGATGAGAGGGAGCC-3′
GAPDH	Human	5′-CTGCCTCGATGGGTGGAGTC-3′	5′-AGGCGCCCAATACGACCAAA-3′
	Rat	5′-AAGGCTGTGGGCAAGGTCAT-3′	5′-TTTCTCCAGGCGGCATGTCA-3′

Table 2
Effect of octreotide on body weight, liver weight and liver index of rats (n = 10, $\bar{X} \pm S$).

Group	Body weight (g)	Liver weight (g)	Liver index
Control	313.20 ± 30.26	8.56 ± 0.54	0.028 ± 0.002
Model	228.80 ± 43.06***	11.77 ± 0.69***	0.053 ± 0.007***
OCT	266.80 ± 36.09#	10.21 ± 0.99##	0.039 ± 0.002###

Compare with Control group: ***P < 0.001; Compare with Model group: #P < 0.05, ##P < 0.01, ###P < 0.001.

antibody at room temperature for 1 h. Then, generally diaminobenzidine (DAB) stained, hematoxylin slightly stained, and neutral balata fixed. Samples were measured by light microscope (Olympus, Tokyo, Japan). The integral optical density (IOD) value of three randomly selected fields at ×200 magnification was quantitatively assessed by using the software of Image-pro plus 6.0 (Media Cybernetics, Inc., Rockville, MD, USA).

2.9. TUNEL assay

Paraffin sections were deparaffinized and in situ detection of the hepatocyte apoptosis in the liver tissues was performed by a fluorescent terminal deoxynucleotidyl transferase dUTP nick-end labeling (TUNEL) assay, according to the manufacturer's instructions (Roche Diagnostics GmbH, Mannheim, Germany). Briefly, following routine dewaxing and treatment with 3% hydrogen peroxide for 20 min, the sections were digested with pepsin for 30 min at 37 °C and treated with TUNEL reaction mixture for 1 h at 37 °C. Hematoxylin dye was used for counterstaining. The average number of apoptotic cells was measured by counting TUNEL-positive nuclei. The number of TUNEL-positive cells in each sample was calculated with ×400 magnification.

2.10. Small interfering RNA transfection

Transfection experiments with small interfering RNA (siRNA) against Bcl-2 and PI3K were performed by using lipofectamine™ 2000 (Invitrogen, USA) according to the manufacture's protocols. Bcl-2 siRNA (sc-29214), PI3K siRNA (sc-61340) and Control siRNA-A (sc-37007) were purchased from Santa Cruz Biotechnology (Danvers, USA). Briefly, LX-2 cells and primary HSCs were cultured in DMEM medium with 10% fetal bovine serum (FBS, Gibco, USA), 100 U/mL penicillin and 100 U/mL streptomycin. After 6 h transfection, the culture medium was changed and TGF-β1 was added. LX-2 cells and primary HSCs were cultured at 37 °C in a humidified atmosphere containing 5% CO_2 incubator for 24 h. The culture medium was changed again and 1×10^{-6} mol/L octreotide was added. After incubator for 24 h, LX-2 cells and primary HSCs were collected for Western blotting.

2.11. Western blotting

The total protein content was extracted from the liver tissues and cells using radio immunoprecipitation assay (RIPA) lysis buffer (Beyotime, China). The protein was separated by a 10% sodium dodecyl sulfate-polyacrylamide (SDS-PAGE) gel electrophoresis and transferred to polyvinylidene fluoride membranes (Millipore Corp, Billerica, MA, USA). After they were blocked with 5% defatted milk for 2 h at room temperature, the membrane was incubated with the specific primary antibodies overnight at 4 °C. Rabbit polyclonal anti-α-SMA (Proteintech, No.55135-1-AP, USA), collagen I (Abcam, ab34710, UK), Bcl-2 (Abcam, ab32124, UK), Bax (Abcam, ab32503, UK), PI3K (Abcam, ab32089, UK), p-PI3K (Abcam, ab182651, UK), AKT (Abcam, ab179463, UK), p-AKT (Abcam, ab38449, UK), caspase3 (Abcam, ab13847, UK) and cleaved-caspase3 (Abcam, ab32042, UK) were diluted 1:500, 1:1000, 1:1000, 1:6000, 1:6000 , 1:600, 1:500, 1:600, 1:500 and 1:500 , respectively. Mouse monoclonal anti-β-actin (Abcam, ab8226, UK) was diluted 1:5000. After washing with TBS/Tween20 buffer, the membranes were then incubated with secondary antibodies for 1 h at room temperature. The special protein bands were developed onto a chemiluminescence western blotting detection system. The protein was visualized with a ECL-chemiluminescent kit (ECL-plus, Thermo Fisher Scientific). The software of Image J was used to analyze the intensity of bands.

2.12. Real-time PCR analysis

Total RNA was extracted from liver tissues and LX-2 cells samples using TRIzol reagents (Invitrogen, USA) according to the manufacture's protocol. A NanoDrop 2000 (Thermo Fisher Scientific) was used to measure concentration and purity of the RNA. The first-strand cDNA synthesis kit (TaKaRa, Shiga, Japan) was used to generate cDNA from total RNA in each sample. Afterward, real-time PCR was conducted in a detection system with SYBR-Green Master Mix (TaKaRa, Shiga, Japan). The relative expression mRNA level of the genes in liver tissues and cells samples was calculated using the $2^{-\Delta\Delta Ct}$ method, normalizing for the expression of housekeeping gene GAPDH. The primer sequences used in this study are shown in Table 1.

2.13. Statistical analysis

All data are represented as means ± SD (standard deviation). The significance of difference was analyzed by One-Way ANOVA or Student's *t*-test using the SPSS 19.0 software (IBM Co., Armonk, NY, USA). Values of $P < 0.05$ are considered to be statistically significant.

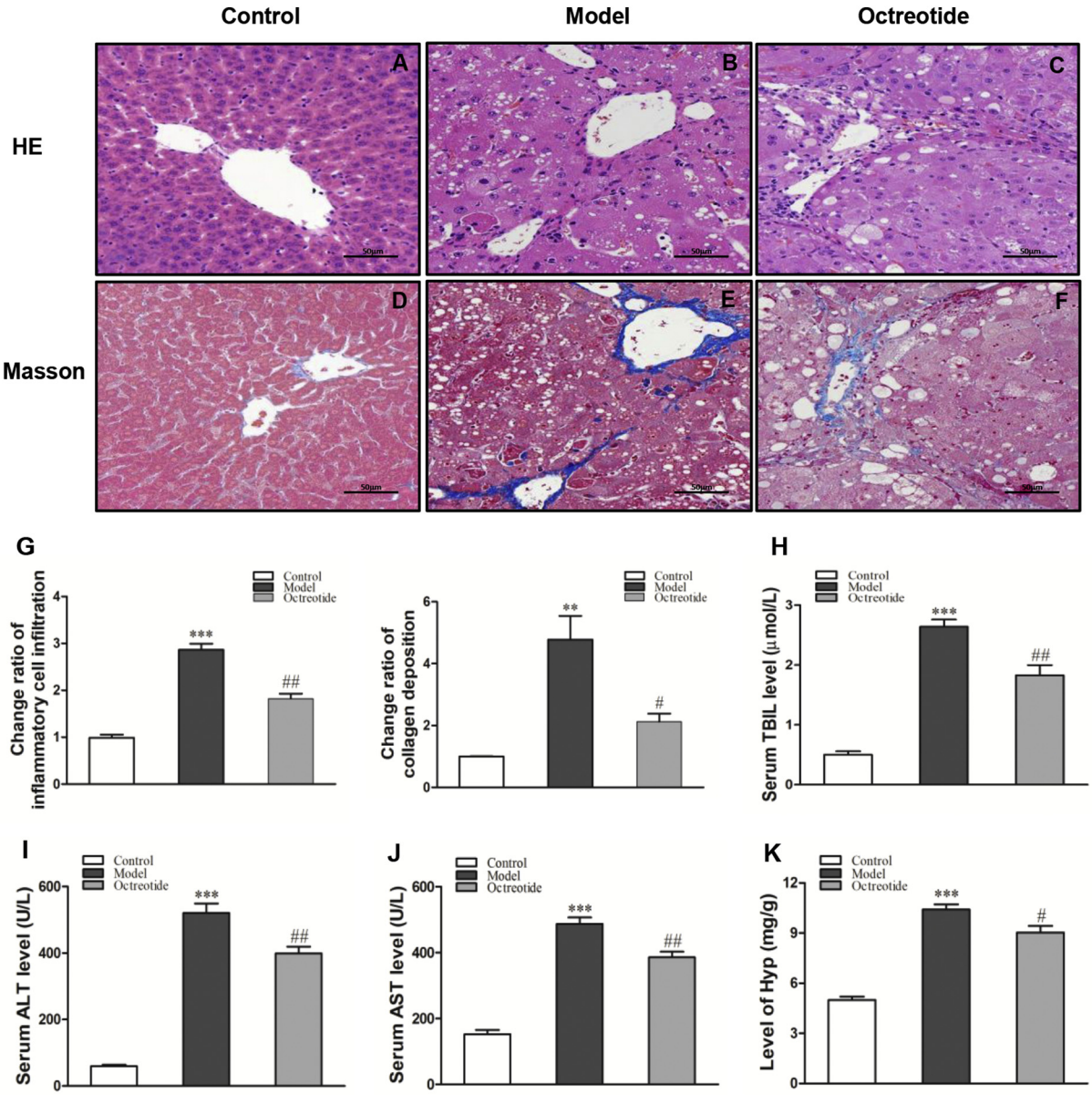

Fig. 1. Octreotide alleviates CCL_4-induced liver injury and fibrosis in rats. (A–C) Hematoxylin and eosin (H&E) staining of rats liver sections (×400); (D–F) Masson staining of rats liver sections (×400); (G) change ratio of inflammatory cell infiltration and collagen deposition of rats liver sections were measured by the software of Image-pro plus 6.0; (H–J) serum concentrations of TBIL, ALT, AST in rats; (K) hydroxyproline (Hyp) content in rat livers. $^{***}P < 0.001$, $^{**}P < 0.01$ versus control group; $^{\#}P < 0.05$, $^{\#\#}P < 0.01$ versus model group.

Table 3
Effect of octreotide on serum concentrations HA, LN, PIIINP and IV-C (n = 10, $\bar{\chi} \pm S$).

Group	HA (U/L)	LN (ng/mL)	PIIINP (ng/mL)	IV-C (ng/mL)
Control	34.12 ± 6.71	13.30 ± 2.69	1.95 ± 0.24	16.23 ± 2.50
Model	214.50 ± 48.48***	128.20 ± 24.04***	5.50 ± 0.93***	107.09 ± 14.48***
OCT	158.60 ± 36.91#	83.16 ± 24.84##	4.18 ± 0.66##	83.14 ± 11.07##

Compare with Control group: $^{***}P < 0.001$; Compare with Model group: $^{\#}P < 0.05$, $^{\#\#}P < 0.01$.

3. Results

3.1. Octreotide alleviates CCl_4-induced liver injury and fibrosis in rats

As shown in Table 2, octreotide treatment significantly increased the body weight of rats in the octreotide group compared to model group ($P < 0.05$). Upon treatment, the liver weight in the octreotide group decreased significantly compared with the model group ($P < 0.01$). The liver index scores rose significantly in the model and octreotide group ($P < 0.001$). A great difference in liver index was observed between the model group and octreotide group.

The histopathological analysis with Hematoxylin & Eosin (H&E) staining and Masson's trichrome staining indicated that the lobular structure was destroyed in the model group, accompanied by extensive hepatic necrosis, inflammatory cell infiltration, bundles of collagen fiber deposition, vacuolated hepatocytes and hyalinization cytoplasm,

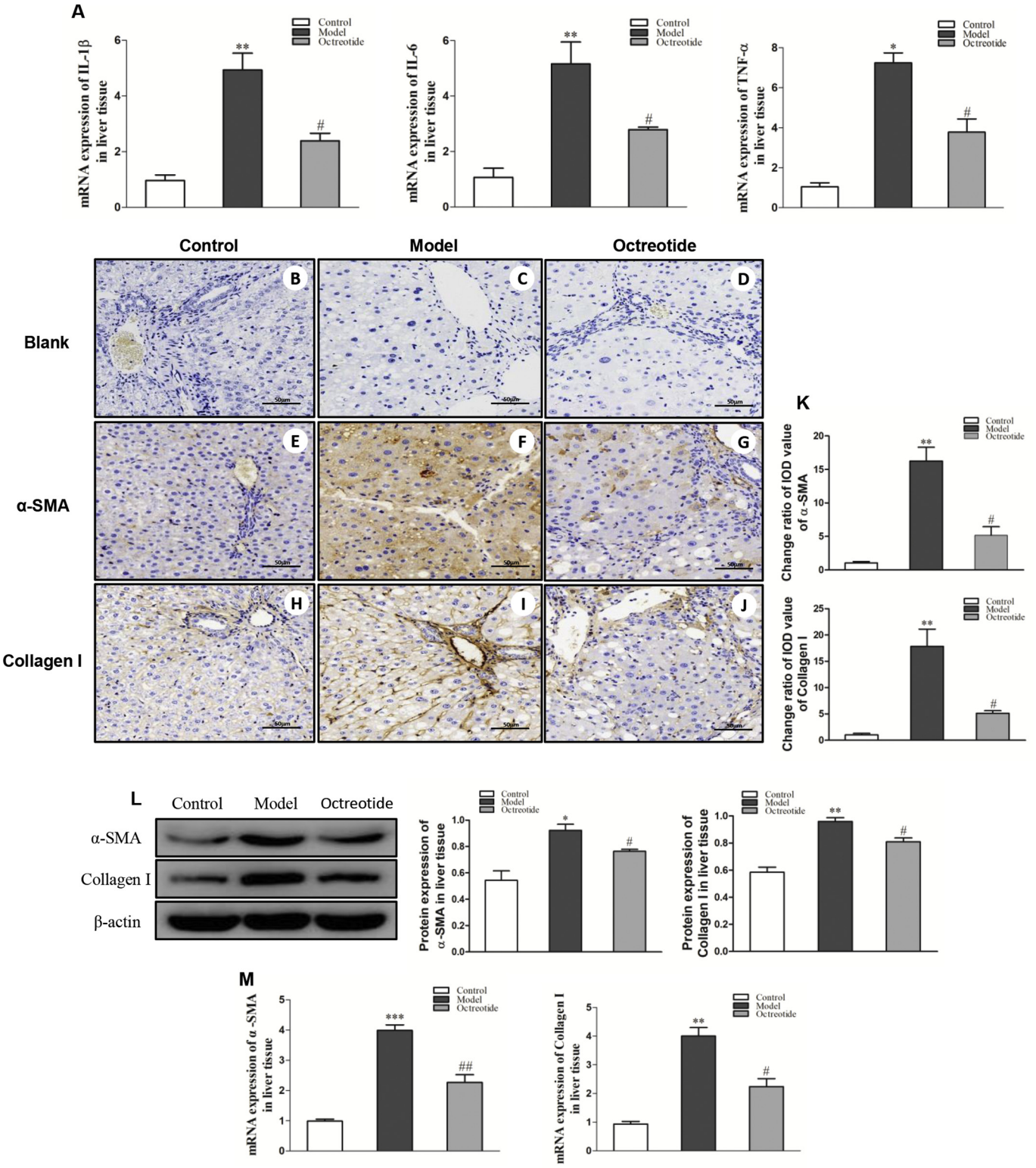

Fig. 2. Octreotide suppresses inflammation and the activation of HSC. (A) Relative mRNA levels of IL-1β, IL-6 and TNF-α in rats liver tissue. (B–D) No primary antibody control was run and showed no detectable staining. Expression of (E–G) α-SMA and (H–J) collagen I were determined by immunohistochemistry (×400); (K) relative integral optical density (IOD) value of the expression of α-SMA and collagen I were measured by the software of Image-pro plus 6.0; (L–M) the protein and mRNA level of α-SMA and collagen I in rats liver tissue were measured by Western blot and Real-time PCR analysis, respectively. $^{*}P < 0.05$, $^{**}P < 0.01$, $^{***}P < 0.001$ versus control group; $^{\#}P < 0.05$, $^{\#\#}P < 0.01$ versus model group.

while no necrosis, inflammation and a few collagen fibers around the central vein were observed in the control group. Treatment with octreotide, however, clearly decreased collagen deposition, inflammatory cell infiltration and vacuolated hepatocytes to improve hepatic architecture and morphology (Fig. 1A–G).

Serum concentrations of TBIL, ALT and AST, compared to the control group, were significantly higher in the model group ($P < 0.001$). Octreotide treatment significantly reduced the levels of TBIL, ALT and

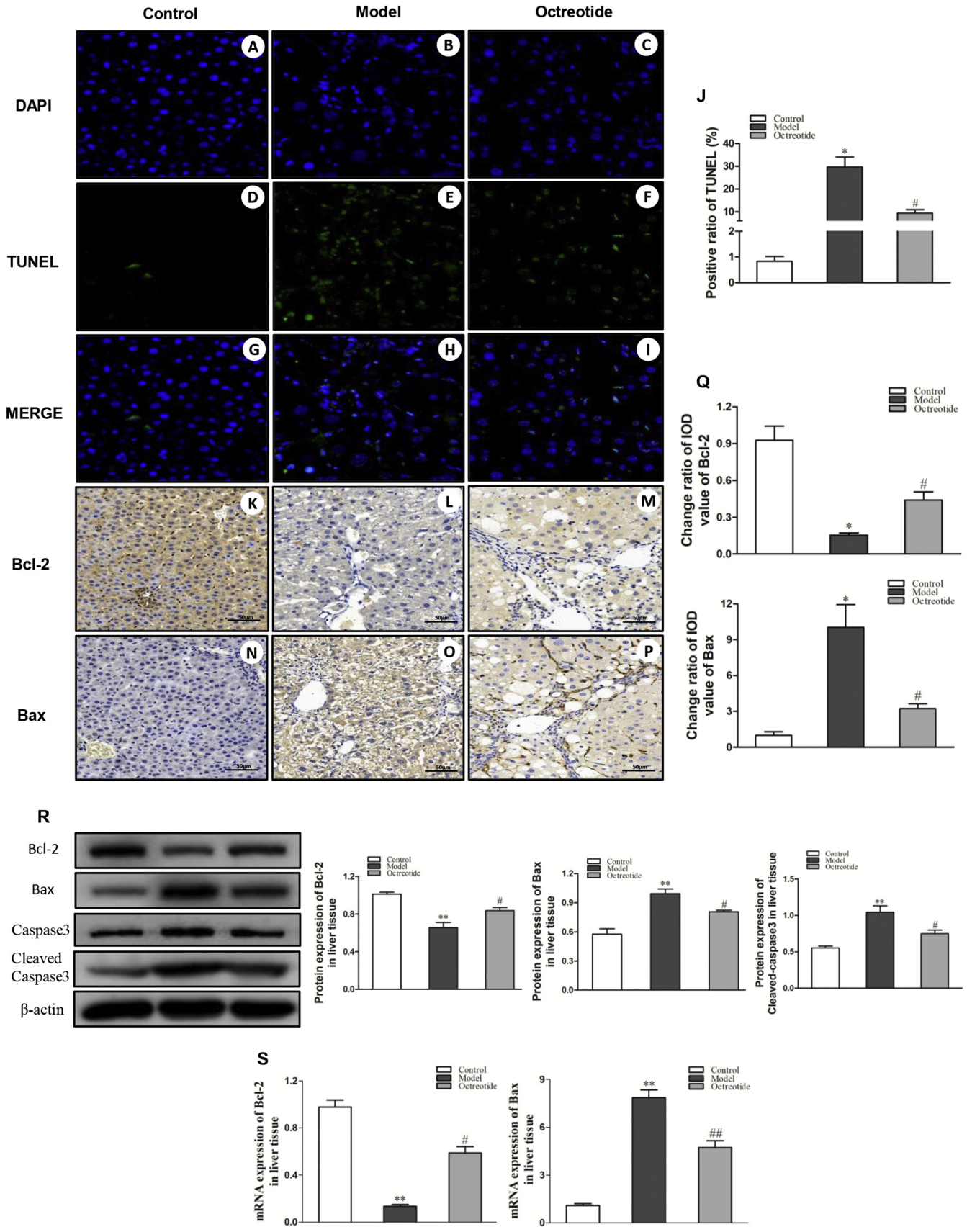

Fig. 3. Octreotide suppresses CCL_4-induced hepatocyte apoptosis via Bcl-2/Bax signaling pathway. (A–C) DAPI staining, (D–F) TUNEL staining and (G–I) MERGE image in rats liver tissue (×400) and (J) the positive ratio of TUNEL staining in the three groups; expression of (K–M) Bcl-2 and (N–P) Bax were determined by immunohistochemistry (×400); (Q) relative integral optical density (IOD) value of the expression of Bax and Bcl-2 were measured by the software of Image-pro plus 6.0. (R–S) The protein and mRNA level of Bax, Bcl-2, Caspase3 and Cleaved Caspase3 in rats liver tissue were measured by Western blot and Real-time PCR analysis, respectively. $^{*}P < 0.05$, $^{**}P < 0.01$ versus control group; $^{\#}P < 0.05$, $^{\#\#}P < 0.01$ versus model group.

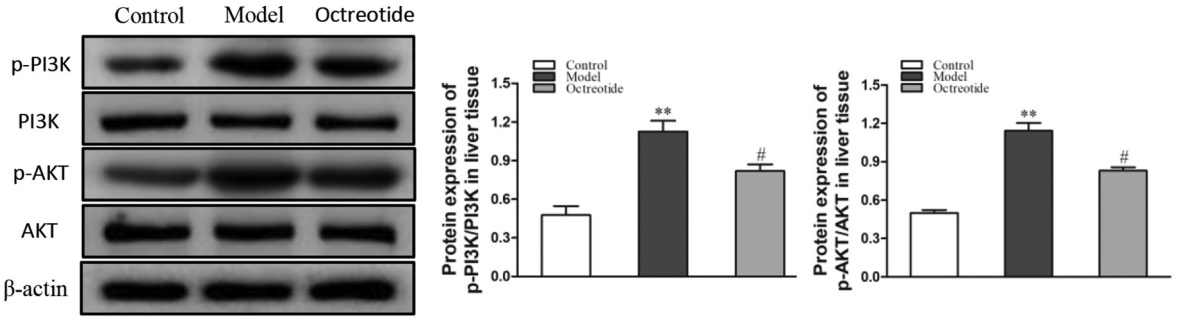

Fig. 4. Octreotide suppresses PI3K/Akt signaling pathway in CCL_4-induced liver fibrosis in rats. The protein level of p-PI3K, PI3K, p-Akt and Akt in rats liver tissue were measured by Western blot. $^{**}P < 0.01$ versus control group; $^{\#}P < 0.05$ versus model group.

AST compared to the model group ($P < 0.01$, Fig. 1H–J). Furthermore, Hyp, the major component of collagen protein, elevated remarkably in the model group compared to the control group ($P < 0.001$) but decreased in the octreotide group compared to the model group ($P < 0.05$, Fig. 1K). In addition, the serum markers of liver fibrosis (HA, LN, IV-C and PIIIP) also increased in the model group, but decreased in the octreotide group ($P < 0.05$, Table 3).

3.2. Octreotide suppresses inflammation and the activation of HSCs in CCl_4-induced liver fibrosis

Levels of inflammatory cytokines (IL-1β, IL-6 and TNF-α) were significantly up-regulated in the model group, while their levels all decreased with octreotide treatment ($P < 0.05$; $P < 0.01$, respectively, Fig. 2A). Furthermore, as shown in Fig. 2E–J, immunohistochemistry analysis revealed that the expression of α-SMA and collagen I were clearly elevated in the model group compared to the control group (15.6-fold of the control group, 17.2-fold of the control group, respectively; $P < 0.01$, Fig. 2K), suggesting that HSCs could activate in CCl_4-induced liver fibrosis in rats. Interestingly, expression of α-SMA and collagen I (5.0-fold of the control group, 4.9-fold of the control group, respectively; $P < 0.05$, Fig. 2K) decreased by the octreotide treatment. Meanwhile, the protein and mRNA expression of α-SMA and collagen I in liver tissues were detected by western blot and qRT-PCR, respectively (Fig. 2L and M). We found that octreotide down-regulated the protein and mRNA expression of α-SMA and collagen I ($P < 0.05$; $P < 0.01$, respectively) in agreement with immunohistochemistry results.

3.3. Octreotide suppresses CCl_4-induced hepatocyte apoptosis via Bcl-2/Bax signaling pathway in fibrotic liver tissues

The hepatocyte apoptosis was evaluated by TUNEL staining (Fig. 3A–I) and the results indicate that a significant increase of hepatocyte apoptosis was found in model group compared to control group ($P < 0.05$). However, the octreotide group shows a significantly smaller number of TUNEL-positive hepatocytes than that of model group ($P < 0.05$). Meanwhile, the protein level of caspase3 and cleaved caspase3 was detected by western blot. As indicated in Fig. 3R, the results shown that the protein level of cleaved caspase3 significantly elevated in the model group ($P < 0.01$), and it reduced by octreotide treatment ($P < 0.05$). However, the expression levels of caspase3 were not significantly different among three groups.

Additionally, apoptosis-associated protein Bcl-2 and Bax were measured by immunohistochemistry. As shown in Fig. 3K–P, the results indicated that compared to control group, the expression level of Bcl-2 decreased in the model group (0.2-fold of the control group, $P < 0.05$, Fig. 3Q), whereas the expression level of Bax elevated in the model group (10.3-fold of the control group, $P < 0.05$, Fig. 3Q). Intriguingly, octreotide treatment up-regulated the expression level of Bcl-2 (0.5-fold of the control group, $P < 0.05$, Fig. 3Q) and down-regulated the expression level of Bax (3.3-fold of the control group, $P < 0.05$, Fig. 3Q), all compared to model group. In addition, western blot and qRT-PCR were used to measure the protein and mRNA expression of Bcl-2 and Bax, and the results were in agreement with immunohistochemistry ($P < 0.05$, Fig. 3R and S).

3.4. Octreotide suppresses PI3K/AKT signaling pathway in CCl_4-induced liver fibrosis

As shown in Fig. 4, compared to the control group, the protein expression of p-PI3K/PI3K and p-AKT/AKT increased in the model group ($P < 0.01$). However, the protein expression of p-PI3K/PI3K and p-AKT/AKT was suppressed by octreotide treatment, compared to the model group ($P < 0.05$), which revealed that octreotide alleviated liver fibrosis by inhibiting the PI3K/AKT signaling pathway. Meanwhile, the expression of PI3K and AKT did not significantly change.

3.5. Octreotide suppresses inflammation and the activation of HSCs in TGF-β1-treated LX-2 cells and primary HSCs

The effects of octreotide on the expression of inflammatory cytokines were detected by qRT-PCR. The results indicated that compared to the normal group, the levels of IL-1β, IL-6 and TNF-α increased in the control group, while their levels all decreased in a dose-dependent manner by octreotide treatment ($P < 0.05$, Fig. 5A). Additionally, the expression of protein and mRNA of α-SMA and collagen I were evaluated by western blot and qRT-PCR, respectively. The protein and mRNA expression of α-SMA and collagen I, compared to the normal group, were higher in the control group ($P < 0.01$, Fig. 5B and C). Octreotide down-regulated protein and mRNA expression of α-SMA and collagen I in a dose dependent manner, compared to in the control group ($P < 0.05$, Fig. 5B and C). As shown in Fig. 5D and E, compared to the siBcl-2 and siPI3K-treated group, the protein expression of α-SMA and collagen I did not significantly changed in siBcl-2, siPI3K and octreotide-treated group.

3.6. Octreotide suppresses the proliferation of activated LX-2 cells via Bcl-2/Bax signaling pathway in vitro

As shown in Fig. 6A, LX-2 cells treated with TGF-β1 were used as controls. The MTT assay showed that octreotide inhibited cell proliferation in a dose-dependent manner ($P < 0.05$). Meanwhile, in order to explore whether octreotide was cytotoxic to LX-2 cells exposed to concentrations of 1×10^{-8}, 1×10^{-7} and 1×10^{-6} mol/L, the MTT assay was used to analyze the cytotoxicity of octreotide, and the results demonstrated that octreotide had no lethal effect on the LX-2 cells ($P > 0.05$, Fig. 6B). Then, images of LX-2 cells exposed to TGF-β1 and octreotide were taken by a phase contrast microscope, and the results revealed that when LX-2 cells treated with TGF-β1, the shape of cells tend to showed fibroblast-like appearances (spindle-like and spread) and high density, and when activated LX-2 cells treated with octreotide,

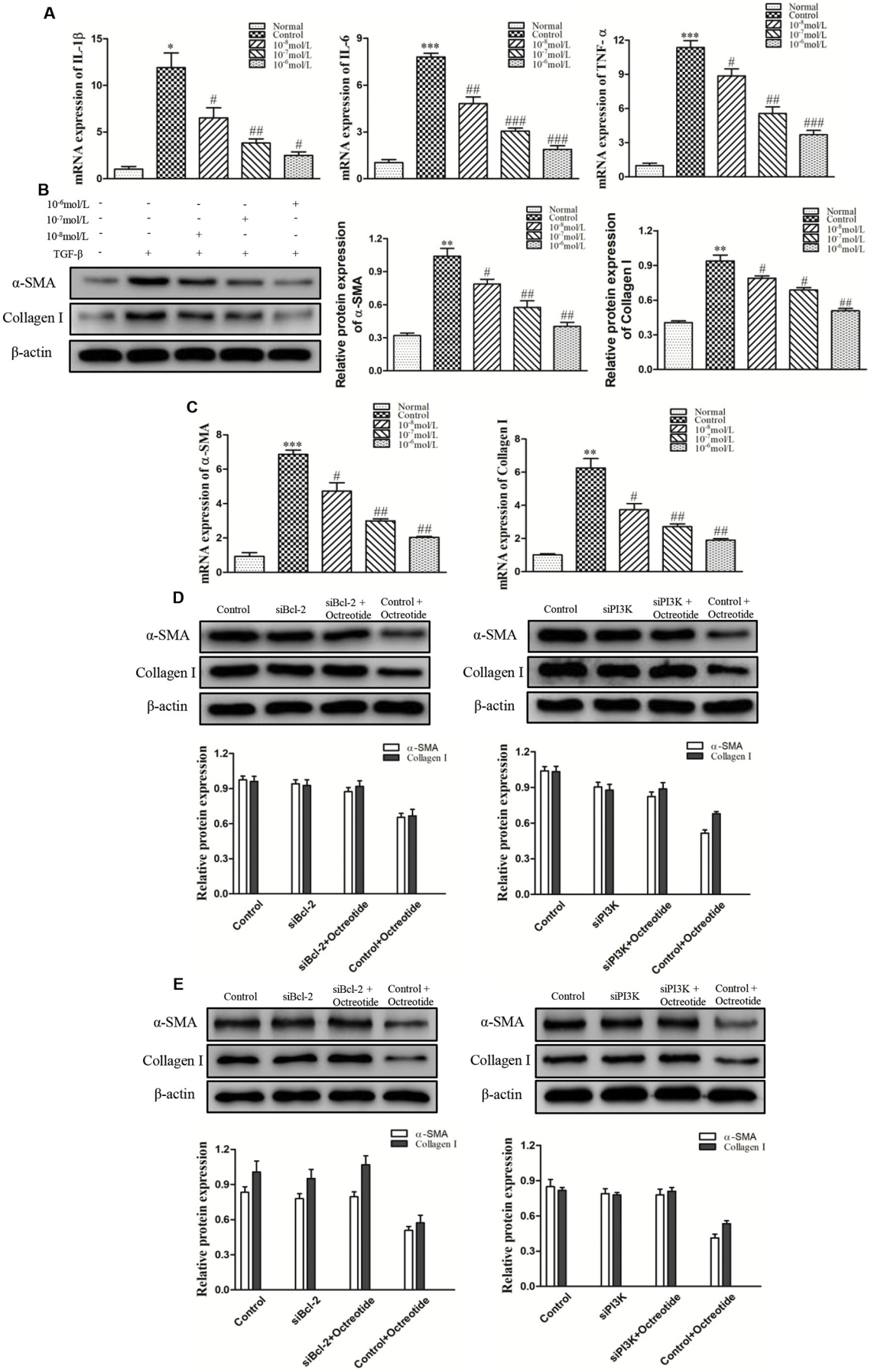

(caption on next page)

Fig. 5. Octreotide suppresses inflammation and the activation of HSCs in TGF-β1-treated LX-2 cells and primary HSCs. (A) Relative mRNA levels of IL-1β, IL-6 and TNF-α in TGF-β1-treated LX-2 cells; (B–C) the protein and mRNA level of α-SMA and collagen I in TGF-β1-treated LX-2 cells were measured by Western blot and Real-time PCR analysis, respectively. (D) The protein level of α-SMA and collagen I in siBcl-2 or siPI3K-treated activated LX-2 cells were measured by Western blot. (E) The protein level of α-SMA and collagen I in siBcl-2 or siPI3K-treated primary HSCs were measured by Western blot. $^{*}P < 0.05$, $^{**}P < 0.01$, $^{***}P < 0.001$ versus control group; $^{\#}P < 0.05$, $^{\#\#}P < 0.01$, $^{\#\#\#}P < 0.001$ versus model group.

the shape of LX-2 cells showed decrease in spread and density (Fig. 6C). Furthermore, as shown in Fig. 6D and E, western blot and qRT-PCR results showed that the protein and mRNA expression of Bcl-2 in the control group significantly increased compared to the normal group ($P < 0.001$). In comparison with the normal group, the protein and mRNA expression of Bax in the control group was markedly decreased ($P < 0.01$). Meanwhile, treatment with octreotide dose-dependently down-regulated the expression of Bcl-2 and increased the expression of Bax compared to control group ($P < 0.05$).

3.7. Octreotide suppresses PI3K/AKT signaling pathway in TGF-β1-treated LX-2 cells

The protein expression levels of p-PI3K, PI3K, p-AKT and AKT were evaluated by western blot. As shown in Fig. 7, the protein expression of p-PI3K/PI3K and p-AKT/AKT in control group increased compared to normal group ($P < 0.001$). Meanwhile, the decrease in p-PI3K/PI3K and p-AKT/AKT was observed following the treatment with octreotide dose-dependently ($P < 0.05$). Collectively, octreotide inhibited the PI3K/AKT signaling pathway in TGF-β1-treated LX-2 cells.

4. Discussion

Liver fibrosis is a consequence of prolonged exposure to several drugs or inflammatory hepatic diseases and can progress to liver cirrhosis or hepatocellular carcinoma [23,24]. The pathology of liver fibrosis is induced by activation of HSCs and massive accumulation of extracellular matrix (ECM). In previous studies, octreotide is reported to alleviate liver fibrosis by reducing the release of inflammatory cytokines [25,26]. The findings of the present study were consistent with those of previous studies and further demonstrate that octreotide alleviates liver fibrosis via multiple pathways, including the inflammatory response, hepatocyte apoptosis, proliferation and activation of HSCs, Bcl-2/Bax signaling pathway and the PI3K/AKT signaling pathway. These results indicated that there would be a potential octreotide antifibrotic therapy in the treatment of hepatic fibrosis.

Serum TBIL, ALT and AST, as markers of hepatotoxicity, reflects the degree of hepatocyte injury [27–29]. When liver cells are stimulated by certain factors to become necrotic, these markers are released into the blood from tissue cells and serve as indicators of liver status. In our study, the results of TBIL, ALT and AST showed that octreotide could alleviate liver injury. Hyp is a constituent of collagen and a marker of collagen deposition [30,31]. Liver Hyp content significantly increased in the model group compared to control group, and significantly decreased in the octreotide treatment group. Serum HA, LN, IV-C and PIIIP are used to evaluate the degree of liver fibrosis [32,33]. With the progression of liver disease, the concentration of HA, LN, IV-C and PIIIP increase and reach the highest levels in liver cirrhosis. The serum levels of HA, LN, IV-C and PIIIP are up-regulated in the model group compared to control group, and markedly down-regulated in the octreotide treatment group. Meanwhile, in line with those results, HE and Masson's staining demonstrated that the liver lobule in the model group was replaced by extensive development of fibrosis and paraplastic connective tissues. Deposition of abnormal excess collagen is characteristic of hepatic fibrosis, and the damage of liver tissues is improved by octreotide. Therefore, octreotide may be a promising treatment for hepatic fibrosis.

Recent studies have reported that activated HSCs could promote the fibrogenic process by stimulating and secreting a wide range of pro-inflammatory cytokines (e.g. IL-1β, IL-6 and TNF-α) [34–36]. These inflammation factors, which induce the fibrotic response and participates in hepatic fibrosis by contributing to the deposition of ECM, may be involved in hepatic fibrosis causing liver tissue injury. In agreement with these findings, octreotide in our study induced a decrease of CCl_4-induced inflammation in vivo and TGF-β1-induced inflammation in vitro to inhibit the progression of liver fibrosis by down-regulating the mRNA expression of IL-1β, IL-6 and TNF-α as a result of CCl_4 and TGF-β1 intoxication.

Furthermore, the activation of HSCs plays an important role in the pathological process of liver fibrosis and has been considered as a target for anti-fibrotic therapy [37–39]. Hepatic fibrosis is characterized by the massive accumulation of ECM, especially collagen I, which is primarily produced by myofibroblasts. HSCs are the major source of myofibroblasts during the procession of liver injury [40]. Myofibroblasts increase the expression of α-SMA that is regarded as a biomarker of activated HSCs [41]. Therefore, activated HSCs are responsible for accumulation and deposition of the majority of massive ECM in the fibrotic liver by up-regulating secretion of α-SMA and collagen I. In this study, the expression levels of α-SMA and collagen I were measured to evaluate the effect of octreotide on HSCs activation by immunohistochemistry, western blot and qRT-PCR. The results clearly demonstrated that octreotide could inhibit HSC activation to attenuate liver fibrosis by down-regulating α-SMA and collagen I.

Apoptosis, a form of cell death, is regulated by multiply molecular signaling pathways, including mitochondrial pathways [42,43]. Hepatocyte apoptosis and activated HSC apoptosis are vital step in the progress of hepatic fibrosis [13,44,45], thus it could be a useful therapeutic target to reverse hepatic fibrosis. The mitochondrial pathway of apoptosis is regulated by the Bcl-2 family of protein, such as Bcl-2 and Bax [46,47]. In our study, the expression levels of Bcl-2, Bax, caspase3 and cleaved caspase3 were detected by immunohistochemistry, western blot and qRT-PCR. The results indicate that octreotide inhibited hepatocyte apoptosis might be dependent on down-regulated Bax and cleaved caspase3; up-regulated Bcl-2, and induced activated HSC apoptosis, accompanying by inhibiting the proliferation of activated HSCs, through increased Bax and a decrease in Bcl-2. Meanwhile, the TUNEL assay was performed to further evaluate the anti-apoptosis effect of octreotide. The results also revealed that apoptosis was induced in numerous hepatocytes in CCl_4-induced liver fibrosis and decreased by octreotide treatment, which is consistent with immunohistochemistry, western blot and qRT-PCR results. Thus, our findings suggested that inhibition of hepatocyte apoptosis and promotion of activated HSC apoptosis could potentially alleviate hepatic fibrosis, and the Bcl-2/Bax signaling pathway would be a target for the anti-fibrosis strategy of octreotide.

Previous studies have revealed that the PI3K/AKT signaling pathway is critical for the progression of hepatic fibrosis, including inhibiting HSC apoptosis, stimulating HSC proliferation and modulating ECM synthesis [48–50]. Activation of PI3K leads to the activation of its key downstream kinase, AKT, thereby regulating cellular activities [11,51]. However, whether octreotide could attenuate liver fibrosis and HSC activation by inhibiting PI3K/AKT signaling pathway remains unclear. Therefore, this study was designed to investigate whether the PI3K/AKT signaling pathway was inhibited by octreotide. The results indicated that the levels of p-PI3K and p-AKT apparently increased in the fibrosis models and significantly decreased after octreotide treatment, suggesting that the anti-hepatic fibrosis effect of octreotide is could be dependent on the suppression of the PI3K/AKT signaling

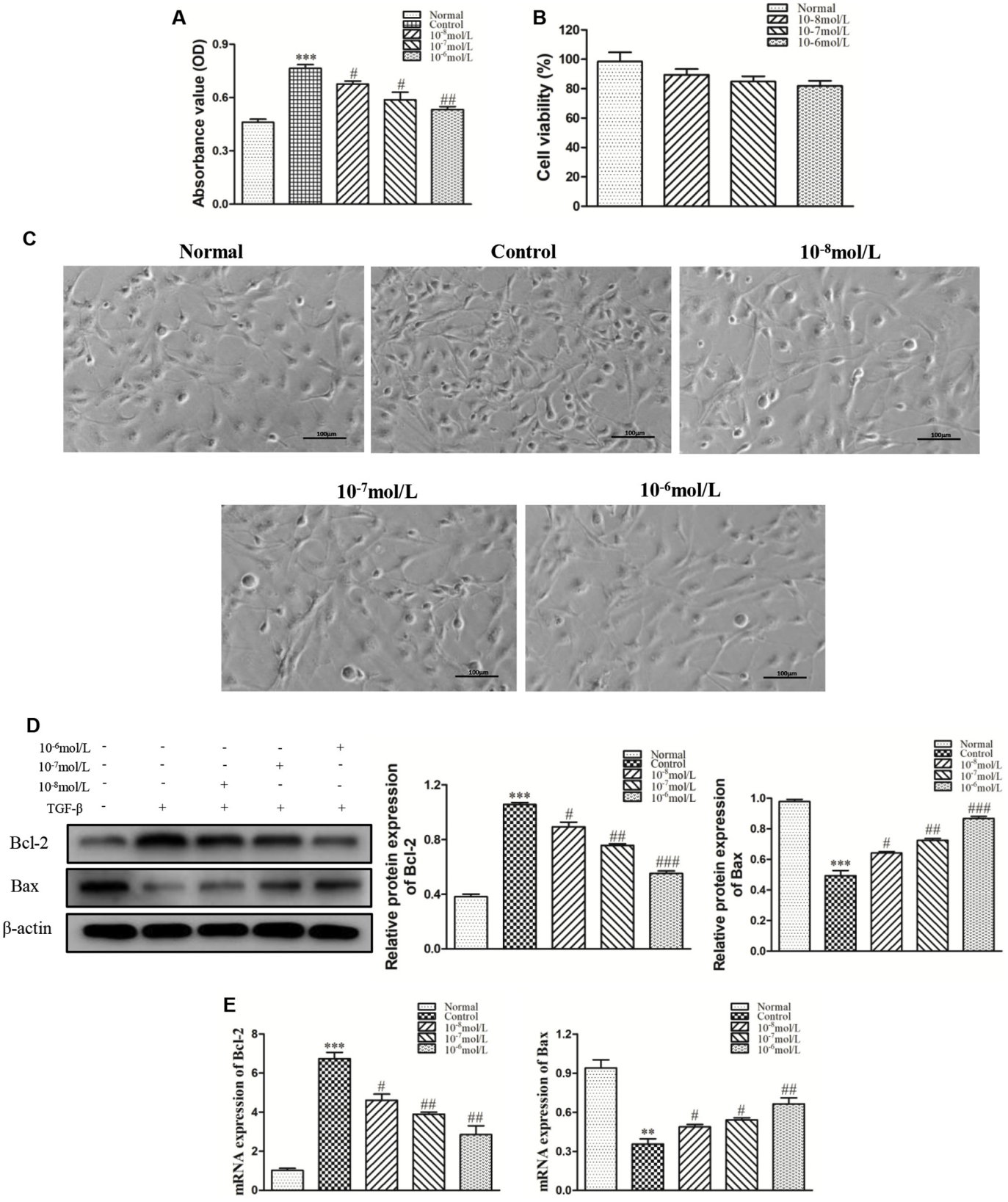

Fig. 6. Octreotide suppresses the proliferation of activated LX-2 cells via Bcl-2/Bax signaling pathway in vitro. (A) Octreotide inhibits the proliferation of activated LX-2 cells in dose-dependent manner measured by MTT assay; (B) octreotide has no effect on the cell viability of LX-2 cells; (C) phase contrast imaging of LX-2 cells (×200); (D–E) the protein and mRNA level of Bcl-2 and Bax in vitro were determined by Western blot and Real-time PCR analysis, respectively. $^{*}P < 0.05$, $^{**}P < 0.01$, $^{***}P < 0.001$ versus normal group; $^{\#}P < 0.05$, $^{\#\#}P < 0.01$, $^{\#\#\#}P < 0.001$ versus control group.

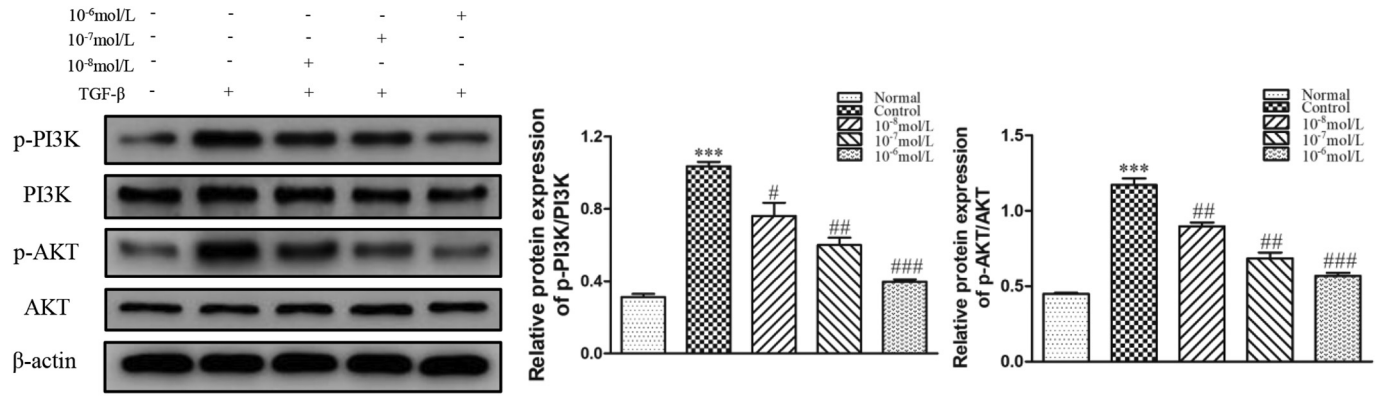

Fig. 7. Octreotide suppresses PI3K/Akt signaling pathway in TGF-β1-treated LX-2 cells. The protein level of p-PI3K, PI3K, p-Akt and Akt in vitro were measured by Western blot. $^{***}P < 0.001$ versus normal group; $^{\#}P < 0.05$, $^{\#\#}P < 0.01$, $^{\#\#\#}P < 0.001$ versus control group.

pathway.

In conclusion, this study indicated that octreotide possessed a therapeutic effect on CCl_4-induced liver fibrosis in vivo and TGF-β1-treated LX-2 cells in vitro. The anti-fibrotic effect of octreotide was associated with multiple mechanisms, including inhibition of inflammation, regulation of Bcl-2/Bax signaling pathway preventing hepatocyte apoptosis and promoting activated HSC apoptosis; and inhibition of HSC activation and ECM synthesis via the suppression of the PI3K/AKT signaling pathway. These results provided the evidence that octreotide has therapeutic potential against hepatic fibrosis and might provide a novel mechanism for the anti-fibrotic effects of octreotide.

Funding

This research was supported by the Natural Science Foundation of Anhui Province (KJ2014A117 and 1908085MH243).

Acknowledgments

The authors thank all participants contributing to this study.

Declaration of competing interest

The authors declare no conflict of interest.

References

[1] R. Bataller, D.A. Brenner, Liver fibrosis [J], J. Clin. Investig. 115 (4) (2005) 1100.
[2] P. Wang, Y. Koyama, X. Liu, J. Xu, H.Y. Ma, S. Liang, et al., Promising therapy candidates for liver fibrosis [J], Front. Physiol. 7 (2016) 47.
[3] J.P. Iredale, A. Thompson, N.C. Henderson, Extracellular matrix degradation in liver fibrosis: biochemistry and regulation [J], Biochim. Biophys. Acta 1832 (7) (2013) 876–883.
[4] X. Li, X. Wang, C. Han, X. Wang, G. Xing, L. Zhou, et al., Astragaloside IV suppresses collagen production of activated hepatic stellate cells via oxidative stress-mediated p38 MAPK pathway [J], Free Radic. Biol. Med. 60 (2013) 168–176.
[5] V. Hernandez-Gea, S.L. Friedman, Pathogenesis of liver fibrosis [J], Annu. Rev. Pathol. 6 (2011) 425–456.
[6] I. Mederacke, C.C. Hsu, J.S. Troeger, P. Huebener, X. Mu, D.H. Dapito, et al., Fate tracing reveals hepatic stellate cells as dominant contributors to liver fibrosis independent of its aetiology [J], Nat. Commun. 4 (2013) 2823.
[7] K. Iwaisako, C. Jiang, M. Zhang, M. Cong, T.J. Moore-Morris, T.J. Park, et al., Origin of myofibroblasts in the fibrotic liver in mice [J], Proc. Natl. Acad. Sci. U. S. A. 111 (32) (2014) E3297–E3305.
[8] E. Seki, R.F. Schwabe, Hepatic inflammation and fibrosis: functional links and key pathways [J], Hepatology 61 (3) (2015) 1066–1079.
[9] G. Son, I.N. Hines, J. Lindquist, L.W. Schrum, R.A. Rippe, Inhibition of phosphatidylinositol 3-kinase signaling in hepatic stellate cells blocks the progression of hepatic fibrosis [J], Hepatology 50 (5) (2009) 1512–1523.
[10] F. Zhang, Z. Zhang, D. Kong, X. Zhang, L. Chen, X. Zhu, et al., Tetramethylpyrazine reduces glucose and insulin-induced activation of hepatic stellate cells by inhibiting insulin receptor-mediated PI3K/AKT and ERK pathways [J], Mol. Cell. Endocrinol. 382 (1) (2014) 197–204.
[11] J. Wang, E.S. Chu, H.Y. Chen, K. Man, M.Y. Go, X.R. Huang, et al., MicroRNA-29b prevents liver fibrosis by attenuating hepatic stellate cell activation and inducing apoptosis through targeting PI3K/AKT pathway [J], Oncotarget 6 (9) (2015) 7325–7338.
[12] D.Q. Zhang, P. Sun, Q. Jin, X. Li, Y. Zhang, Y.J. Zhang, et al., Resveratrol regulates activated hepatic stellate cells by modulating NF-kappaB and the PI3K/Akt signaling pathway [J], J. Food Sci. 81 (1) (2016) H240–H245.
[13] E. Novo, F. Marra, E. Zamara, L. Valfre di Bonzo, L. Monitillo, S. Cannito, et al., Overexpression of Bcl-2 by activated human hepatic stellate cells: resistance to apoptosis as a mechanism of progressive hepatic fibrogenesis in humans [J], Gut 55 (8) (2006) 1174–1182.
[14] Y. Wang, R. Wang, Y. Wang, R. Peng, Y. Wu, Y. Yuan, Ginkgo biloba extract mitigates liver fibrosis and apoptosis by regulating p38 MAPK, NF-kappaB/IkappaBalpha, and Bcl-2/Bax signaling [J], Drug design, development and therapy 9 (2015) 6303–6317.
[15] Y.T. Hsu, R.J. Youle, Nonionic detergents induce dimerization among members of the Bcl-2 family [J], J. Biol. Chem. 272 (21) (1997) 13829–13834.
[16] A. Canbay, A. Feldstein, E. Baskin-Bey, S.F. Bronk, G. Gerken, G.J. Gores, 22 The caspase inhibitor IDN-6556 attenuates hepatic injury and fibrosis in the bile duct ligated mouse [J], Journal of Pharmacology & Experimental Therapeutics 40 (3) (2004) 1191–1196.
[17] M.E. Guicciardi, G.J. Gores, Apoptosis as a mechanism for liver disease progression [J], Semin. Liver Dis. 30 (4) (2010) 402–410.
[18] G. Chen, Y. Wang, M. Li, T. Xu, X. Wang, B. Hong, et al., Curcumol induces HSC-T6 cell death through suppression of Bcl-2: involvement of PI3K and NF-κB pathways [J], European Journal of Pharmaceutical Sciences Official Journal of the European Federation for Pharmaceutical Sciences 65 (2014) 21–28.
[19] G. Tahan, F. Eren, O. Tarçin, H. Akin, V. Tahan, Ş. H, et al., Effects of a long-acting somatostatin analogue, lanreotide, on bile duct ligation-induced liver fibrosis in rats [J], Turk. J. Gastroenterol. 21 (3) (2010) 287–292.
[20] S.H. Song, X.S. Leng, T. Li, Z.Z. Qin, J.R. Peng, L. Zhao, et al., Expression of subtypes of somatostatin receptors in hepatic stellate cells [J], World J. Gastroenterol. 10 (11) (2004) 1663–1665.
[21] J. Wang, L. Wang, G. Song, B. Han, The mechanism through which octreotide inhibits hepatic stellate cell activity [J], Mol. Med. Rep. 7 (5) (2013) 1559–1564.
[22] C. Zhang, X.Q. Liu, H.N. Sun, X.M. Meng, Y.W. Bao, H.P. Zhang, et al., Octreotide attenuates hepatic fibrosis and hepatic stellate cells proliferation and activation by inhibiting Wnt/beta-catenin signaling pathway, c-Myc and cyclin D1 [J], Int. Immunopharmacol. 63 (2018) 183–190.
[23] T.L. Pan, P.W. Wang, Explore the molecular mechanism of apoptosis induced by tanshinone IIA on activated rat hepatic stellate cells [J], Evidence-based complementary and alternative medicine: eCAM 2012 (2012) 734987.
[24] A. Forner, J.M. Llovet, J. Bruix, Hepatocellular carcinoma [J], Lancet 379 (9822) (2012) 1245–1255.
[25] S. Klironomos, G. Notas, O. Sfakianaki, F. Kiagiadaki, C. Xidakis, E. Kouroumalis, Octreotide modulates the effects on fibrosis of TNF-alpha, TGF-beta and PDGF in activated rat hepatic stellate cells [J], Regul. Pept. 188 (2014) 5–12.
[26] A. Lang, E. Sakhnini, H.H. Fidder, Y. Maor, S. Bar-Meir, Y. Chowers, Somatostatin inhibits pro-inflammatory cytokine secretion from rat hepatic stellate cells [J], Liver international: official journal of the International Association for the Study of the Liver 25 (4) (2005) 808–816.
[27] N. Tang, Y. Zhang, Z. Liu, T. Fu, Q. Liang, X. Ai, Correlation analysis between four serum biomarkers of liver fibrosis and liver function in infants with cholestasis [J], Biomedical reports 5 (1) (2016) 107–112.
[28] J. Woodford, G.D. Shanks, P. Griffin, S. Chalon, J.S. McCarthy, The dynamics of liver function test abnormalities after malaria infection: a retrospective observational study [J], The American journal of tropical medicine and hygiene 98 (4) (2018) 1113–1119.
[29] Y.R. Wang, R.T. Hong, Y.Y. Xie, J.M. Xu, Melatonin ameliorates liver fibrosis induced by carbon tetrachloride in rats via inhibiting TGF-beta1/Smad signaling pathway [J], Current medical science 38 (2) (2018) 236–244.
[30] R. Verma, L. Kushwah, D. Gohel, M. Patel, T. Marvania, S. Balakrishnan, Evaluating the ameliorative potential of quercetin against the bleomycin-induced pulmonary fibrosis in Wistar rats [J], Pulmonary medicine 2013 (2013) 921724.

[31] M.G. Elsakkar, M.M. Eissa, W.A. Hewedy, R.M. Nassra, S.F. Elatrebi, Sodium valproate, a histone deacetylase inhibitor, with praziquantel ameliorates Schistosoma mansoni-induced liver fibrosis in mice [J], Life Sci. 162 (2016) 95–101.
[32] K. Zhang, Y. Gao, M. Zhong, Y. Xu, J. Li, Y. Chen, et al., Hepatoprotective effects of Dicliptera chinensis polysaccharides on dimethylnitrosamine-induced hepatic fibrosis rats and its underlying mechanism [J], J. Ethnopharmacol. 179 (2016) 38–44.
[33] T. Wang, X. Zhou, H. Liu, J. Wang, P. Zhang, Y. Zhu, et al., Fuzheng Huayu capsule as an adjuvant treatment for HBV-related cirrhosis: a systematic review and meta-analysis [J], Phytother. Res. 32 (10) (2017).
[34] D.H. Lu, X.Y. Guo, S.Y. Qin, W. Luo, X.L. Huang, M. Chen, et al., Interleukin-22 ameliorates liver fibrogenesis by attenuating hepatic stellate cell activation and downregulating the levels of inflammatory cytokines [J], World J. Gastroenterol. 21 (5) (2015) 1531–1545.
[35] S. Ceccarelli, N. Panera, M. Mina, D. Gnani, C. De Stefanis, A. Crudele, et al., LPS-induced TNF-alpha factor mediates pro-inflammatory and pro-fibrogenic pattern in non-alcoholic fatty liver disease [J], Oncotarget 6 (39) (2015) 41434–41452.
[36] S. Robert, T. Gicquel, A. Bodin, V. Lagente, E. Boichot, Characterization of the MMP/TIMP imbalance and collagen production induced by IL-1beta or TNF-alpha release from human hepatic stellate cells [J], PLoS One 11 (4) (2016) e0153118.
[37] M.A.A. Atallah, S.M. Elaidy, M.K. Tawfik, Assessment of the possible roles of SB-269970 versus ketanserin on carbon tetrachloride-induced liver fibrosis in rats: oxidative stress/TGF-beta1-induced HSCs activation pathway [J], Pharmacological reports: PR 70 (3) (2018) 509–518.
[38] G. Nguyen, S.Y. Park, C.T. Le, W.S. Park, D.H. Choi, E.H. Cho, Metformin ameliorates activation of hepatic stellate cells and hepatic fibrosis by succinate and GPR91 inhibition [J], Biochem. Biophys. Res. Commun. 495 (4) (2018) 2649–2656.
[39] D.D. Xu, X.F. Li, Y.H. Li, Y.H. Liu, C. Huang, X.M. Meng, et al., TIPE2 attenuates liver fibrosis by reversing the activated hepatic stellate cells [J], Biochem. Biophys. Res. Commun. 498 (1) (2018) 199–206.
[40] J. Xu, X. Liu, Y. Koyama, P. Wang, T. Lan, I.G. Kim, et al., The types of hepatic myofibroblasts contributing to liver fibrosis of different etiologies [J], Front. Pharmacol. 5 (2014) 167.
[41] J.S. Kim, S. Koppula, M.J. Yum, G.M. Shin, Y.J. Chae, S.M. Hong, et al., Anti-fibrotic effects of Cuscuta chinensis with in vitro hepatic stellate cells and a thioacetamide-induced experimental rat model [J], Pharm. Biol. 55 (1) (2017) 1909–1919.
[42] C. Brenner, L. Galluzzi, O. Kepp, G. Kroemer, Decoding cell death signals in liver inflammation [J], J. Hepatol. 59 (3) (2013) 583–594.
[43] T. Luedde, N. Kaplowitz, R.F. Schwabe, Cell death and cell death responses in liver disease: mechanisms and clinical relevance [J], Gastroenterology 147 (4) (2014) 765–783 (e4).
[44] C.C. Li, C.Z. Yang, X.M. Li, X.M. Zhao, Y. Zou, L. Fan, et al., Hydroxysafflor yellow A induces apoptosis in activated hepatic stellate cells through ERK1/2 pathway in vitro [J], European journal of pharmaceutical sciences: official journal of the European Federation for Pharmaceutical Sciences 46 (5) (2012) 397–404.
[45] F. Zhang, D.S. Kong, Z.L. Zhang, N. Lei, X.J. Zhu, X.P. Zhang, et al., Tetramethylpyrazine induces G0/G1 cell cycle arrest and stimulates mitochondrial-mediated and caspase-dependent apoptosis through modulating ERK/p53 signaling in hepatic stellate cells in vitro [J], Apoptosis: an international journal on programmed cell death 18 (2) (2013) 135–149.
[46] Y. Qu, W.H. Chen, L. Zong, M.Y. Xu, L.G. Lu, 18alpha-Glycyrrhizin induces apoptosis and suppresses activation of rat hepatic stellate cells [J], Medical science monitor: international medical journal of experimental and clinical research 18 (1) (2012) BR24–32.
[47] H. Kalkavan, D.R. Green, MOMP, cell suicide as a BCL-2 family business [J], Cell Death Differ. 25 (1) (2018) 46–55.
[48] S. Reif, A. Lang, J.N. Lindquist, Y. Yata, E. Gabele, A. Scanga, et al., The role of focal adhesion kinase-phosphatidylinositol 3-kinase-akt signaling in hepatic stellate cell proliferation and type I collagen expression [J], J. Biol. Chem. 278 (10) (2003) 8083–8090.
[49] C. Guo, L. Xu, Q. He, T. Liang, X. Duan, R. Li, Anti-fibrotic effects of puerarin on CCl4-induced hepatic fibrosis in rats possibly through the regulation of PPAR-gamma expression and inhibition of PI3K/Akt pathway [J], Food and chemical toxicology: an international journal published for the British Industrial Biological Research Association. 56 (2013) 436–442.
[50] R. Peng, S. Wang, R. Wang, Y. Wang, Y. Wu, Y. Yuan, Antifibrotic effects of tanshinol in experimental hepatic fibrosis by targeting PI3K/AKT/mTOR/p70S6K1 signaling pathways [J], Discov. Med. 23 (125) (2017) 81–94.
[51] Q. Chen, L. Chen, X. Wu, F. Zhang, H. Jin, C. Lu, et al., Dihydroartemisinin prevents liver fibrosis in bile duct ligated rats by inducing hepatic stellate cell apoptosis through modulating the PI3K/Akt pathway [J], IUBMB Life 68 (3) (2016) 220–231.